Sensors and Actuators A 304 (2020) 111855

Contents lists available at ScienceDirect

Sensors and Actuators A: Physical

journal homepage: www.elsevier.com/locate/sna

Enhanced piezoelectric tactile sensing behaviors of high-density and low-damage CF_4-plasma-treated IGZO thin-film transistors coated by P(VDF-TrFE) copolymers

Jer-Chyi Wang[a,b,c,*], Yi-Pei Jiang[a], Chi-Hung Lin[d], Shun-Hsiang Chan[d], Ming-Chung Wu[d,e,**]

[a] Department of Electronic Engineering, Chang Gung University, Guishan Dist., 33302, Taoyuan, Taiwan
[b] Department of Neurosurgery, Chang Gung Memorial Hospital, Linkou, Guishan Dist., 33305, Taoyuan, Taiwan
[c] Department of Electronic Engineering, Ming Chi University of Technology, Taishan Dist., 24301, New Taipei City, Taiwan
[d] Department of Chemical and Materials Engineering, Chang Gung University, Guishan Dist., 33302, Taoyuan, Taiwan
[e] Division of Neonatology, Department of Pediatrics, Chang Gung Memorial Hospital, Linkou, Guishan Dist., 33305, Taoyuan, Taiwan

ARTICLE INFO

Article history:
Received 15 October 2019
Received in revised form 7 January 2020
Accepted 19 January 2020
Available online 22 January 2020

Keywords:
Indium gallium zinc oxide (IGZO)
CF_4 plasma
Thin film transistor
Poly(vinylidene fluoride-co-trifluoroethylene) (P(VDF-TrFE))
Piezoelectric
Tactile sensor

ABSTRACT

Piezoelectric pressure sensing behaviors of high-density and low-damage CF_4-plasma-treated indium gallium zinc oxide (IGZO) thin-film transistors (TFTs) coated by poly(vinylidene fluoride-co-trifluoroethylene) (P(VDF-TrFE)) films have been investigated. The CF_4 plasma treatment was performed on the IGZO channel by using an inductively coupled plasma (ICP) system with a quartz filter. Prior to the fabrication of devices, X-ray diffractometer (XRD) and atomic force microscopy (AFM) were applied to identify the enhancement in the crystallinity of P(VDF-TrFE) films on the plasma-fluorinated IGZO films. With the analyses of X-ray photoelectron spectroscopy (XPS), it is proved that the fluorine radicals reacted with the metal-oxygen bonds will increase the oxygen vacancies in IGZO films, contributing to an enhancement in field effect mobility (μ_{FE}) and drain current (I_{DS}) of IGZO TFTs. Furthermore, the fluorine atoms diffused from the IGZO channel into the bottom SiO_2 layer were confirmed by secondary ion-mass spectroscopy (SIMS), reducing the interfacial and oxide charges of the devices for a negative shift in threshold voltage (V_t). Under a 0.5-kg applied force press/release cyclic test, a 4.8-fold increase in drain current response of 1-min CF_4-plasma-treated piezoelectric pressure sensors was optimized, because of the enhanced electrical behaviors of IGZO TFTs and an increase in aligned dipole moments of P(VDF-TrFE) copolymers. The promising results make the piezoelectric pressure sensors with high-density and low-damage CF_4-plasma-treated IGZO TFTs coated by P(VDF-TrFE) copolymer suitable for future high-performance tactile sensing applications.

1. Introduction

Piezoelectricity is a well-known energy conversion technology by transforming mechanical stress into electrical signal, extremely important for the applications in energy harvesting, sensing and actuation [1–3]. Through the integration of piezoelectric devices with some specific modules, the functional piezoelectric system can be used in nanogenerator, electric cigarette lighter, robotic skin, human healthcare, acoustic-electric guitars, piezoelectric motor, and so on [4–9]. Traditionally, inorganic materials such as $Pb(Zr,Ti)O_3$ (PZT) show a high piezoelectric coefficient value of about 400 pC/N, which is approximately one order of magnitude larger than that of the organic materials [10]. Here, polyvinylidenefluoride (PVDF) has been used because of the environmental friendliness and low processing temperatures, attracting substantial interest in biomedicine and flexible electronics [11]. The crystalline forms of α-, β-, γ-, δ-, and ε-phases are observed in PVDF, altered by the fabricating process such as annealing, blending, and mechanical stretching [12–14]. Although α-phase is the most thermodynamically favorable chain conformation, it is non-polar and needs to be converted into polar β-phase for a larger spontaneous polarization. Thus, the highly crystalline β-phase of

* Corresponding author at: Department of Electronic Engineering, Chang Gung University, Guishan Dist., 33302, Taoyuan, Taiwan.
** Corresponding author at: Department of Chemical and Materials Engineering, Chang Gung University, Guishan Dist., 33302, Taoyuan, Taiwan.
E-mail addresses: jcwang@mail.cgu.edu.tw (J.-C. Wang), mingchungwu@cgu.edu.tw (M.-C. Wu).

https://doi.org/10.1016/j.sna.2020.111855
0924-4247/

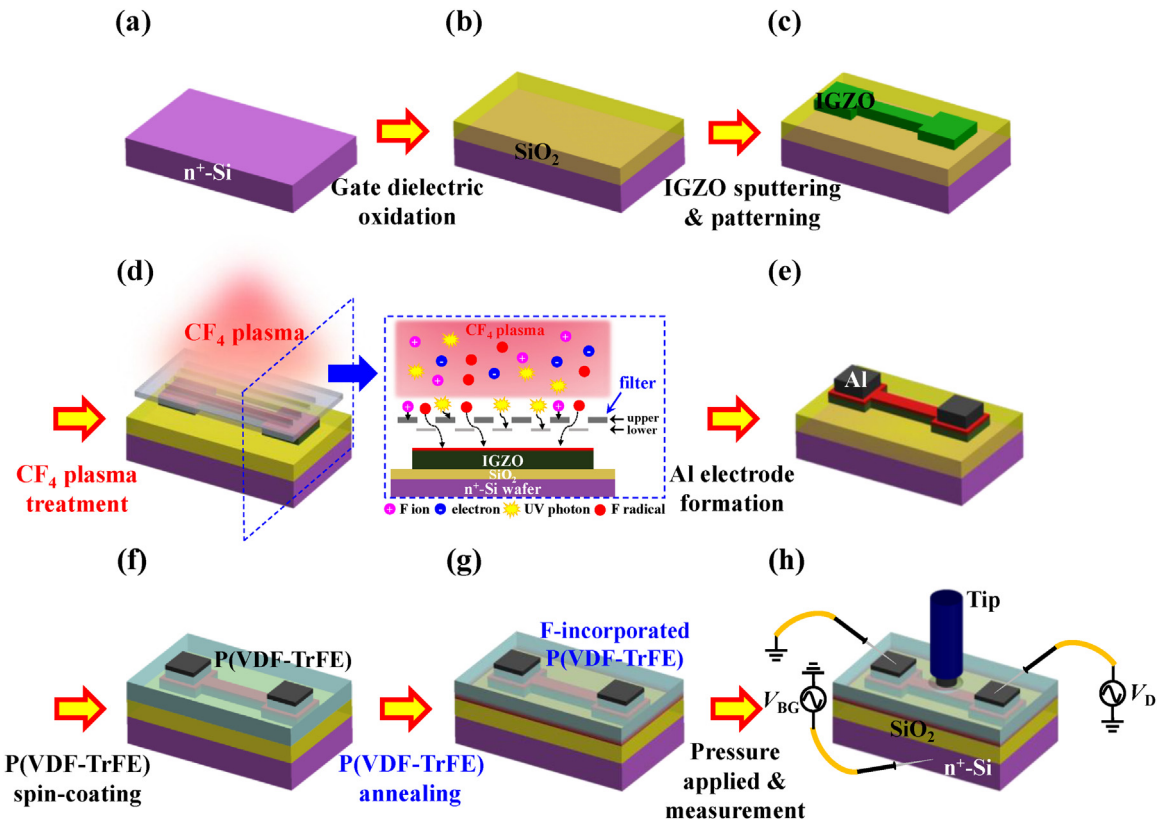

Fig. 1. Fabrication procedures of the piezoelectric pressure sensors with high-density and damage-free CF_4-plasma-treated IGZO TFTs coated by piezoelectric P(VDF-TrFE) copolymers. (a) n^+-Si (100) wafers with standard RCA clean, (b) SiO_2 gate dielectric oxidation in a horizontal furnace at 850 °C, (c) IGZO deposition in dc sputtering system to form the channel material, (d) high-density and damage-free CF_4 plasma treatment on IGZO channels in an inductively coupled plasma (ICP) system with a quartz filter, (e) Al electrode formation at source and drain regions to finish the IGZO TFTs, (f) spin-coating of P(VDF-TrFE) copolymers, (g) thermal annealing at 130 °C for 2 h on the hot plate, and (h) force applied through a tip on P(VDF-TrFE) copolymers to measure the current response of piezoelectric pressure sensors.

PVDF is required and the trifluoroethylene (TrFE) is blended into PVDF to form the P(VDF-TrFE) for better piezoelectric properties [15–18]. To further enhance the piezoelectric behaviors of P(VDF-TrFE) copolymers, the low-temperature solvent vapor annealing, bilayer poly(methyl methacrylate) (PMMA)/P(VDF-TrFE) structure, and the incorporation of nanosized insulating and conductive fillers have been implemented [19–23].

To evaluate the characteristics of piezoelectric materials and apply the films in pressure sensing, bottom-gated thin-film transistors (TFTs) are the most commonly used devices with the piezoelectric film coated on the topside of the channel [24–26]. It is reported that the amorphous InGaZnO (a-IGZO) film has been considered as a promising TFT channel material due to its high mobility, high transparency, and low-temperature process [27–29], compared to those of the silicon-based materials. Recently, some researchers suggested that the performance of IGZO TFTs can be enhanced by the modification of IGZO film composition, the reduction of contact resistance, and plasma treatment [30–35]. For the H_2 plasma treatment, it can passivate the oxygen vacancies and induce the carriers of shallow donors of IGZO TFTs [32]. However, the hydrogen intrusion into the interior of IGZO thin films will degrade the conductive nature, which can be recovered and lessened by the N_2O plasma [33]. In addition, the Ar plasma can reduce the trap density between gate insulator and IGZO channel and the contact resistance between the Pt/Ti source/drain electrode and IGZO channel, respectively, increasing the on-current of TFTs [34]. Huang et al. performed the CHF_3 and O_2 mixed plasma on back channel of IGZO and dielectric/IGZO interface to eliminate the metal-hydroxyl (M–OH) defects induced by the moisture absorption in air for the improved stability of device performances under positive-gate-bias-stress (PGBS) [35]. Nevertheless, with the traditional plasma system, the generation efficiency of plasma is extremely low and the plasma damage on IGZO TFTs is quite serious [36,37]. Up to now, a high-density and low-damage plasma has not yet been treated on IGZO films and the impacts of plasma fluorination on piezoelectric pressure sensors with P(VDF-TrFE)-coated IGZO TFTs have not been explored. In this study, the piezoelectric pressure sensing properties of high-density and low-damage CF_4-plasma-treated IGZO TFTs with P(VDF-TrFE) film coated on the topside of IGZO channel are investigated. The material natures of plasma-fluorinated IGZO layers and P(VDF-TrFE) films on IGZO are identified by X-ray photoelectron spectroscopy (XPS) binding analysis, secondary ion mass spectroscopy (SIMS) depth profiles, X-ray diffractometer (XRD) patterns, and atomic force microscopy (AFM) images. In addition to the improvement in basic electrical behaviors of IGZO TFTs, a significant enhancement in drain current response of the high-density and low-damage CF_4-plasma-treated piezoelectric pressure sensors under a vertical force applied on P(VDF-TrFE) copolymers is proposed, demonstrating the superior piezoelectric pressure sensing behaviors for future applications of P(VDF-TrFE)-coated IGZO TFTs in tactile sensors.

2. Experimental

2.1. Sample preparation

Piezoelectric pressure sensors with high-density and low-damage CF_4-plasma-treated IGZO TFTs coated by P(VDF-TrFE) copolymers were prepared. After the RCA cleaning of the back-gate (BG) n^+-Si wafers, a 50-nm-thick SiO_2 film was thermally grown as

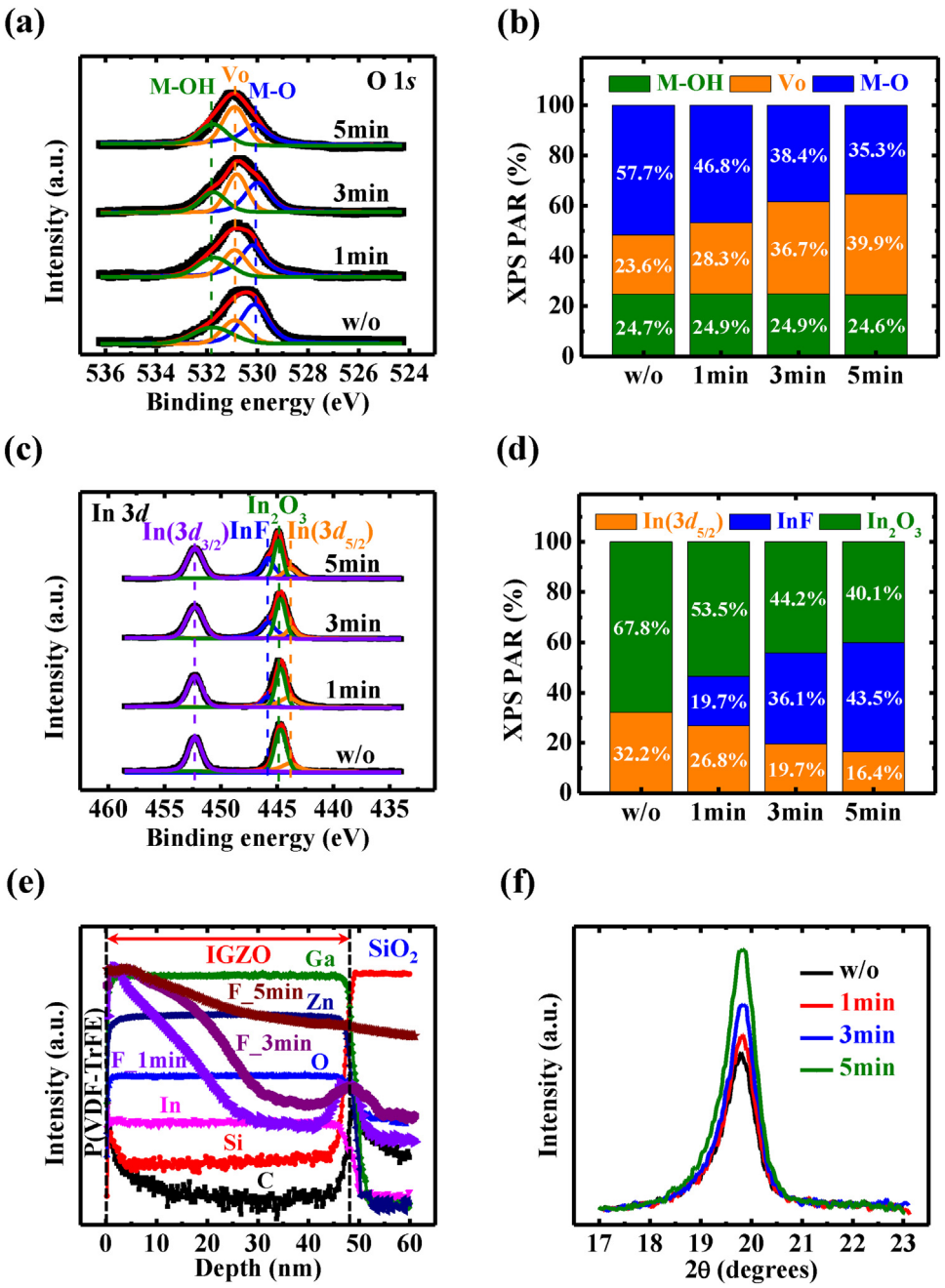

Fig. 2. (a) O 1*s* XPS spectra at film surface of the IGZO films under different CF_4 plasma treatment times. (b) XPS peak-area-ratios (PARs) of metal-oxygen bonds (M–O), oxygen vacancies (Vo) and metal-hydroxyl bonds (M–OH) of these samples. (c) In 3*d* XPS spectra at film surface of the IGZO films under different CF_4 plasma treatment times. (d) XPS PARs of indium atoms ($In(3d_{3/2})$), indium–oxygen bonds (In_2O_3) and indium-fluorine bonds (InF) of these samples. (e) SIMS depth profiles of the IGZO/SiO_2 stacked structure under different CF_4 plasma treatment times. (f) XRD spectra of the P(VDF-TrFE) copolymers on the CF_4-plasma-treated IGZO films.

the dielectric material in a horizontal furnace at 850 °C (Fig. 1(a) and (b)). Then, the samples were subjected to the dc sputtering chamber for the deposition of IGZO films as channel materials. To remove the native surface oxide of the target, the sputtering system was first pumped down to the background pressure of 10^{-5} Torr and a 3-inch IGZO target with stoichiometric In:Ga:Zn:O ratio of 1:1:1:4 (99.99% purity) was pre-cleaned for 10 min by the argon plasma. After that, a 50-nm-thick IGZO layer was deposited via dc sputtering using the argon plasma (dc power of 100 W, argon gas flow of 20 sccm and gas pressure of 6 mTorr) and patterned by a shadow mask with a channel width of 1 mm, as shown in Fig. 1(c). After the active area had been formed, a high-density and low-damage CF_4 plasma treatment was performed on IGZO thin films at a radio-frequency (rf) power of 100 W for 1, 3 and 5 min by using an inductively coupled plasma (ICP) system (KD-ICP/RIE, KaoDuen Tech. Corp., Taiwan) with a quartz filter. The filter was used to block ultra-violet (UV) photons and ions, and only the neutral and highly-reactive fluorine radicals were treated on IGZO films (Fig. 1(d)), as proposed in our previous study on nonvolatile memories [38]. The operating pressure of the chamber and the gas flow of the CF_4 ambient were 300 mTorr and 300 sccm, respectively. Next, a 120-nm-thick Al film was deposited by a thermal evaporator at 10^{-6} Torr with a pure Al bullet (99.999% purity) and patterned by a lift-off process to form the source and drain contacts at a distance of 3.5 mm, as shown in Fig. 1(e). For the material synthesis, the P(VDF-TrFE) powder (70:30 mol %) provided by Piezotech S.A.S., France was dis-

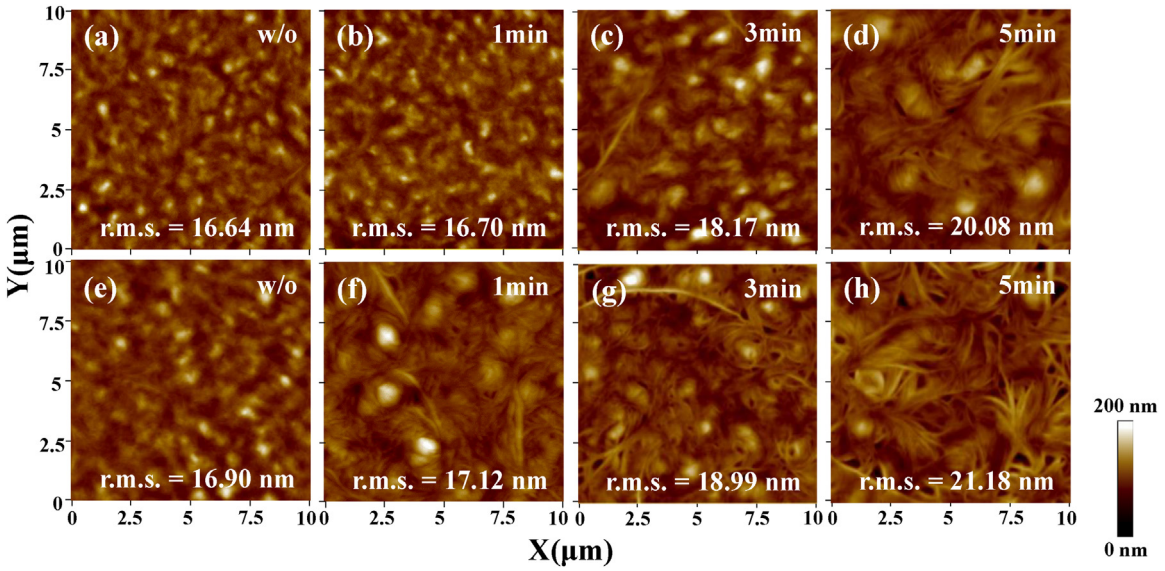

Fig. 3. AFM topographic images of the P(VDF-TrFE) copolymers on the (a,e) untreated and (b,f) 1-, (c,g) 3-, and (d,h) 5-min CF_4-plasma-treated IGZO films before and after annealing, respectively. The surface roughness (r.m.s.) measured by topographic images was noted in these figures.

solved in dimethylformamide (DMF) at a concentration of 5.0 wt. %. The solution was spin-coated on the plasma-fluorinated IGZO TFTs at 750 rpm for 30 s in a glove box (Fig. 1(f)). An appropriate shear stress from spin-coating procedure can improve the dipole moment alignment of P(VDF-TrFE) copolymers [39]. The thickness of P(VDF-TrFE) films measured by ellipsometry was approximately 350 nm. After the piezoelectric films had been formed, all samples were baked at 120 °C to dry the films and then annealed at 130 °C for 2 h on a hot plate to induce the crystallinity of the P(VDF-TrFE) films (Fig. 1(g)), especially the β-phase, so as to order the electric dipoles to obtain piezoelectricity [40]. Finally, the piezoelectric P(VDF-TrFE) films were patterned by photolithography to open the source and drain areas for probing. The entire fabrication procedures of the piezoelectric pressure sensors with high-density and low-damage CF_4-plasma-treated IGZO TFTs coated by P(VDF-TrFE) copolymers were illustrated in Fig. 1(a)-(g).

2.2. Characterization of materials and devices

Following the CF_4 plasma treatment, the surface morphology of IGZO layers and P(VDF-TrFE) films before and after crystallization was investigated by using a Bruker AXS MultiMode8 AFM system (Bruker AXS GmbH, Germany). The composition and chemical bonds of IGZO films under different CF_4 plasma treatment conditions were detected by SIMS depth profiling using a TOF-SIMS V system (ION-TOF GmbH, Germany) and XPS using a VG ESCA scientific theta probe spectrometer (Thermo Fisher Scientific Inc., USA) with a pass energy of 50 eV at a take-off angle of 53° and Al Kα (1486.6 eV) radiation as the excitation source, respectively. Furthermore, the crystallinity of P(VDF-TrFE) films on the plasma-fluorinated IGZO layers was examined by XRD using a Bruker D2 phaser system (Bruker AXS GmbH, Germany) with Cu Kα (8.04 keV) radiation as the excitation source. To realize the diffusion of fluorine atoms from the plasma-fluorinated IGZO films to the P(VDF-TrFE) copolymers, the XPS analysis was also performed on P(VDF-TrFE) films. For the characterization of piezoelectric pressure sensors with IGZO TFTs coated by P(VDF-TrFE) films, the force was applied using a MAX-1KN-H automatic load tester (Japan Instrumentation System Co., Ltd., Japan) equipped with a force gauge. A tip size of 2 mm in diameter, larger than that of the channel width, was used to apply an equal vertical force of 0.1 – 0.5 kg, as illustrated in Fig. 1(h). The drain current versus back-gate voltage (I_{DS}–V_{BG}) and drain current versus drain voltage (I_{DS}–V_{DS}) curves of the plasma-fluorinated IGZO TFTs were measured using a Keithley 4200 semiconductor characterization system (Tektronix, Inc., USA).

3. Results and discussion

3.1. Material analyses of IGZO films and P(VDF-TrFE) copolymers on IGZO

Fig. 2(a) shows the O 1*s* XPS spectra at film surface of the IGZO films under different CF_4 plasma treatment times. The spectra can be deconvoluted into three components, *i.e.* metal-oxygen bonds (530.1 eV), oxygen vacancies (530.9 eV) and metal-hydroxyl bonds (531.8 eV) [41]. The peak-area-ratios (PARs) of all deconvoluted spectra were calculated and are summarized in Fig. 2(b). It is worthy to note that the PARs of oxygen vacancies (Vo) and metal-oxygen bonds (M–O) increase and decrease, respectively, owing to the reaction of highly-reactive fluorine radicals with M–O bonds [42]. The increased amount of fluorine incorporation into the IGZO films with an increase in high-density CF_4 plasma treatment time was examined by the F 1*s* XPS spectra and is demonstrated in Fig. S1. On the other hand, the PARs of metal-hydroxyl bonds (M–OH) keep the same for the IGZO films under different CF_4 plasma treatment times because the IGZO layers are protected by the hydrophobic P(VDF-TrFE) films to avoid the moisture absorption, which can be confirmed by the similar behavior of O 1*s* spectra at the depth of 10 nm from the IGZO film surface (Fig. S2). Fig. 2(c) presents the In 3*d* XPS spectra of the IGZO films under different CF_4 plasma treatment times. In this figure, the sub-spectra of In $3d_{5/2}$ consisted of three components, which can be assigned to indium atoms (443.8 eV), indium–oxygen bonds (444.9 eV) and indium-fluorine bonds (445.9 eV), respectively [43–46]. To identify the influences of high-density CF_4 plasma treatment on IGZO films, the PARs of all deconvoluted spectra were calculated and are summarized in Fig. 2(d). For the films with CF_4 plasma treatment, the peak of indium-fluorine bonds (InF) occurs and the PAR increases with an increase in plasma treatment time as a result of the increased amount of highly-reactive fluorine radicals (Fig. S1), leading to a decrease in PARs of indium atoms (In($3d_{3/2}$)) and indium–oxygen bonds (In_2O_3). The same trending can be observed for the Ga 2*p*

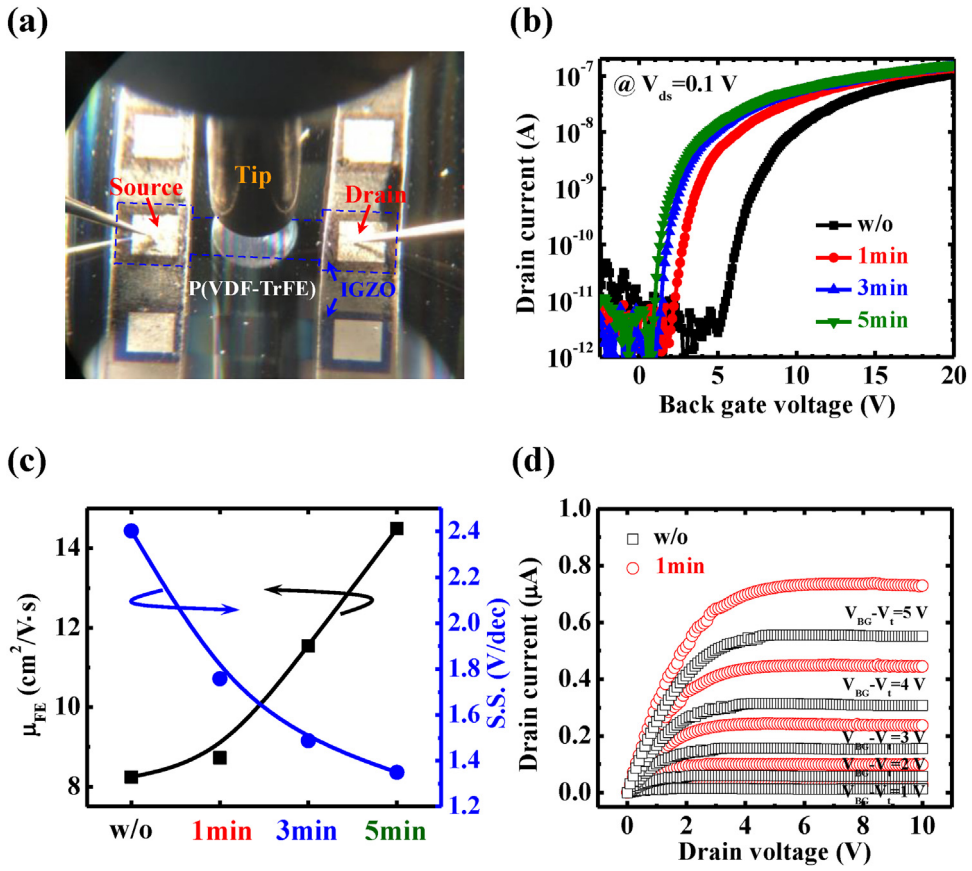

Fig. 4. (a) Optical microscopy (OM) image of the IGZO TFTs coated by the P(VDF-TrFE) copolymers for the piezoelectric pressure testing. (b) Typical I_{DS}–V_{BG} transfer characteristics at V_{DS} = 0.1 V of the IGZO TFTs with and without CF_4 plasma treatment. The back gate bias was swept from –2.5 to 20 V. (c) Dependence of CF_4 plasma treatment time on field-effect mobility (μ_{FE}) and subthreshold slope (S.S.) of IGZO TFTs. (d) Output characteristics of untreated and 1-min CF_4-plasma-treated IGZO TFTs measured at V_{BG} – V_t = 1 to 5 V.

and Zn 2*p* XPS spectra as shown in Figs. S3 and S4 respectively. Fig. 2(e) exhibits the SIMS depth profiles of the IGZO/SiO_2 stacked structure under different CF_4 plasma treatment times. It can be observed that the fluorine atoms have diffused to the IGZO/SiO_2 interface and further into the SiO_2 dielectrics. In addition, more fluorine atoms are incorporated into the IGZO and SiO_2 layers with longer CF_4 plasma treatment time, passivating the defects at the IGZO/SiO_2 interface and in the SiO_2 dielectrics, which will be discussed later. Fig. 2(f) shows the XRD spectra of the P(VDF-TrFE) copolymers on the plasma-fluorinated IGZO films. The XRD patterns illustrate that the high-density CF_4 plasma treatment on IGZO films has a strong effect on the crystallinity in P(VDF-TrFE) as shown by the changes in the intensity of the peak at $2\theta \approx 20^\circ$. With an increase in CF_4 plasma treatment time, the β-phase of P(VDF-TrFE) films is remarkably enhanced. Furthermore, the C 1*s* XPS spectra of the P(VDF-TrFE) copolymers on the plasma-fluorinated IGZO films before and after the annealing process are shown in Fig. S5. The spectra at film surface of the P(VDF-TrFE) copolymers can be deconvoluted into four peaks at the binding energies of 286.3, 287, 288.7, and 291.2 eV for C-H_2, C–F, C—FH, and C-F_2 bonds, respectively [47]. To realize the diffusion of fluorine atoms, the PARs of the fluorine-related deconvoluted spectra, *i.e.* C–F, C—FH and C-F_2 bonds, with respect to the C-H_2 bond before and after the annealing process were calculated and are illustrated in inset of Fig. S5. For the samples without annealing, the PARs of the P(VDF-TrFE) films are almost the same. On the other hand, after the annealing process, the PARs gradually increase with an increase in CF_4 plasma treatment time, indicating the diffusion of fluorine atoms from the high-density CF_4 plasma-treated IGZO films to the P(VDF-TrFE) copolymers.

Topographic images of the untreated and high-density CF_4-plasma-treated IGZO films with a field of view of 10 μm × 10 μm were collected and are shown in the plot of the surface roughness (r.m.s.) in Fig. S6. A negligible roughness change (0.44–1.67 nm) is observed on IGZO films before and after the plasma treatment, implying a low-damage plasma treatment system with a quartz filter. After the spin-coating of the P(VDF-TrFE) films on IGZO layers, the surface roughness of the P(VDF-TrFE) films is approximately 16–20 nm, as shown in Fig. 3(a)-(d). Subsequently, all films were annealed to induce the crystallinity and the topographic images of these films were examined and are presented in Fig. 3(e)-(h). In these images, the dark and bright areas are identified as the amorphous and crystalline portions respectively, as proposed by Solnyshkin et al. [48]. Compared with that of the P(VDF-TrFE) copolymer on the untreated one, the crystalline fraction of the films on the high-density CF_4-plasma-treated IGZO layers increases dramatically. Additionally, the change in the r.m.s. values of the P(VDF-TrFE) films before and after annealing is significantly increased with an increase in CF_4 plasma treatment time. It is suggested that the rougher surface of the P(VDF-TrFE) copolymers can be ascribed to the improved crystallinity [49], meaning that the high-density CF_4 plasma treatment on IGZO layers can enhance the crystallinity in P(VDF-TrFE) films, as revealed in the XRD patterns of Fig. 2(f).

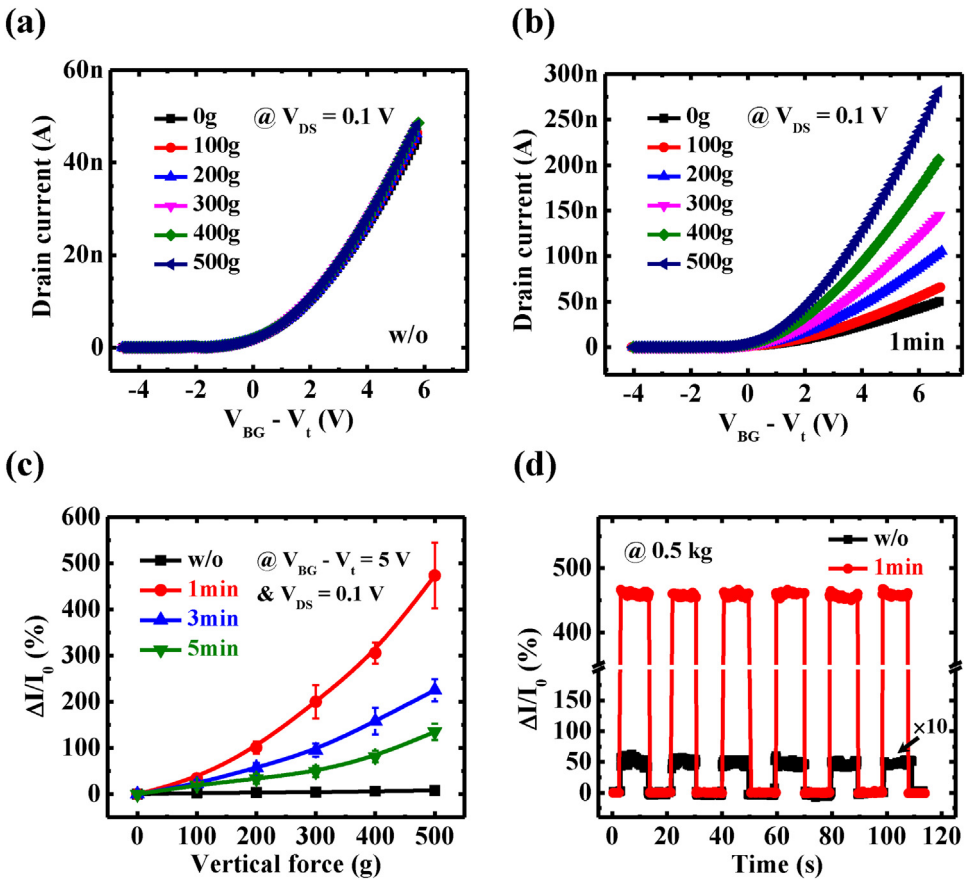

Fig. 5. I_{DS}–V_{BG} characteristics of (a) untreated and (b) 1-min CF_4-plasma-treated piezoelectric pressure sensors before and after applying a vertical force. The force was ranged from 0.1 to 0.5 kg. (c) Statistical distributions of the current response of the CF_4-plasma-treated piezoelectric pressure sensors after applying different forces. At least 20 samples were measured for each of the force applied. (d) Time-dependent current response of the piezoelectric pressure sensors without and with CF_4 plasma treatment for 1 min during a press/release cyclic test. The current was measured at $V_{BG} - V_t = 5$ V and $V_{DS} = 0.1$ V under the force applied at 0.5 kg for 10 s and then released for 10 s repeatedly.

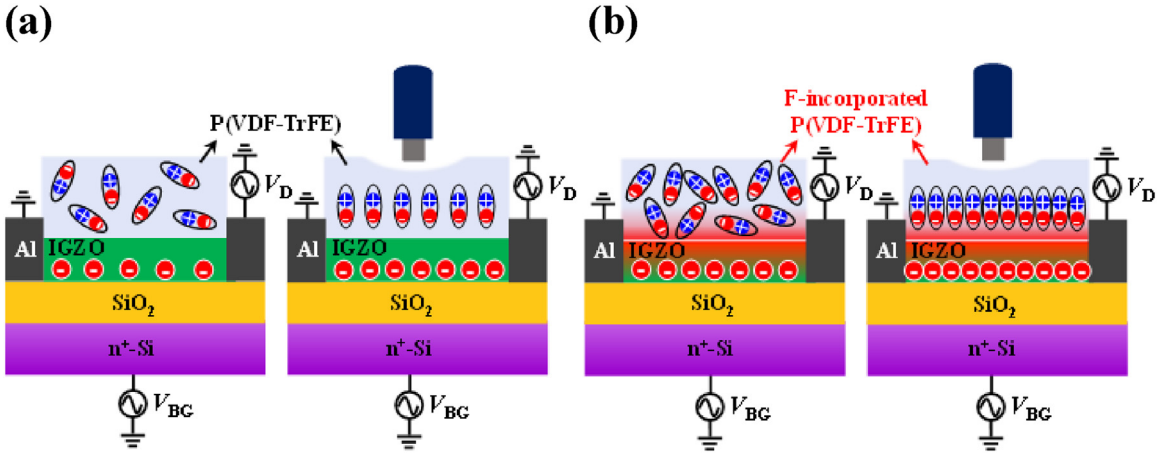

Fig. 6. The schematic diagrams of (a) untreated and (b) CF_4-plasma treated piezoelectric pressure sensors with IGZO TFTs coated by P(VDF-TrFE) copolymers before and after the force applied, respectively.

3.2. Electrical behaviors of piezoelectric pressure sensors with IGZO TFTs coated by P(VDF-TrFE) copolymers

Fig. 4(a) shows the optical microscopy (OM) image of the IGZO TFTs coated by P(VDF-TrFE) copolymers for the piezoelectric pressure testing. It is clearly observed that the tip is placed at the center of the channel to effectively offer the piezoelectric dipole moments of the P(VDF-TrFE) film on the IGZO channel. Fig. 4(b) presents the typical I_{DS}–V_{BG} transfer characteristics at $V_{DS} = 0.1$ V of the IGZO TFTs with and without CF_4 plasma treatment. The back gate bias was swept from –2.5 to 20 V. For the IGZO TFTs with CF_4 plasma treatment on the channel, a significant threshold voltage (V_t) shift toward the negative direction is observed, which can be ascribed to the passivation of defects at the IGZO/SiO_2 interface and in the SiO_2 gate dielectrics by the high-density and low-damage CF_4 plasma treatment [50,51]. Thus, the subthreshold slope (S.S.) of the IGZO

TFTs with an increase in high-density CF_4 plasma treatment time decreases from 2.4 to 1.35 V/dec, as shown in Fig. 4(c). Further, the field-effect mobility (μ_{FE}) of the devices increases from 8.24 to 14.5 cm^2/V·s due to the reduction of charges in SiO_2 gate dielectrics and an increase in oxygen vacancies of IGZO films [52], as shown in Fig. 2(b). After the coating of piezoelectric P(VDF-TrFE) copolymers on the CF_4-plasma-treated IGZO TFTs, there is no obvious change in transfer characteristics, as shown in Fig. S7. In order to investigate the drive current (I_{DS}), the output characteristics of these samples were measured at $V_{BG} - V_t$ = 1 to 5 V and are shown in Fig. 4(d) and Fig. S8 respectively. It can be found that the CF_4 plasma treatment can effectively enhance the drive capability of IGZO TFTs because of an increase in carrier mobility, as presented in Fig. 4(c).

Fig. 5(a) and (b) and Fig. S9 demonstrate the I_{DS}–V_{BG} characteristics of the piezoelectric pressure sensors with IGZO TFTs coated by P(VDF-TrFE) copolymers before and after applying a vertical force. The force was ranged from 0.1 to 0.5 kg. Compared with that of the samples without a force applied, the drain current of the sensors increases with an increase in the force applied. It is reported that the current modulation with respect to the force applied of the piezoelectric pressure sensors can be attributed to the charge generated from the piezoelectric P(VDF-TrFE) copolymers [53], as formulated by $Q = d_{33} \times F$, where Q is the charge generated from the piezoelectric dipoles, d_{33} is the piezoelectric coefficient and F is the force applied on P(VDF-TrFE) films. Specially, the sensors with a longer CF_4 plasma treatment time exhibit a larger enhancement in drain current under a force applied, which can be referred to the improved crystallinity in the fluorine-incorporated P(VDF-TrFE) copolymers for more piezoelectric charges generated, as shown in Fig. 2(f). Here, the current response, which is considered as the current modulation normalized by the initial drain current, can be calculated according to the following equation [54],

$$\text{Current response} = \left(\frac{I - I_0}{I_0}\right) \times 100\% = \left(\frac{\Delta I}{I_0}\right) \times 100\% \quad (1)$$

where I_0 and I are the drain current of the piezoelectric pressure sensors measured at V_{BG}–V_t = 5 V and V_{DS} = 0.1 V without and with a force applied on P(VDF-TrFE) copolymers respectively. The statistical distributions of the current response of the piezoelectric pressure sensors after applying different forces were calculated from the I_{DS}–V_{BG} transfer characteristics and are presented in Fig. 5(c). At least 10 samples were measured for each of the force applied. For the untreated piezoelectric pressure sensors, the current response is only 5.6% after applying a force of 0.5 kg. On the other hand, for the samples with CF_4 plasma treatment for 1 min, a significant increment in current response of the piezoelectric pressure sensors is obtained, achieving ~ 480% under a 0.5-kg force. As the CF_4 plasma treatment time increases to more than 3 min, the current response of the sensors is reduced, due to the higher drain current of the IGZO TFTs under a longer CF_4 plasma treatment time, as revealed in the output characteristics of Fig. 4(d) and Fig. S8. Fig. 5(d) shows the time-dependent current response of the piezoelectric pressure sensors without and with CF_4 plasma treatment for 1 min during a press/release cyclic test. The current was measured at V_{BG}–V_t = 5 V and V_{DS} = 0.1 V under the force applied at 0.5 kg for 10 s and then released for 10 s repeatedly. To show the curves on the same scale, a multiplication factor of ten had to be used in the current response of the sensors without treatment. A high current response and repetitive press/release test of the piezoelectric pressure sensors with CF_4 plasma treatment for 1 min is obtained, suitable for future high-efficient tactile sensors. Fig. 6(a) and (b) show the schematic diagrams of the untreated and CF_4-plasma-treated piezoelectric pressure sensors with IGZO TFTs coated by P(VDF-TrFE) copolymers respectively before and after the force applied. P(VDF-TrFE) is a crystalline copolymer in which monomer units of PVDF (–CH_2-CF_2-) and TrFE (-CF_2-CFH-) are connected. However, there are some defects and imperfections within the P(VDF-TrFE) chains, leading to the capture of charges and hindering the switchable polarization. For a P(VDF-TrFE) copolymer on the CF_4-plasma-treated IGZO channel, the fluorine atoms diffused from the IGZO film to the P(VDF-TrFE) copolymer during annealing (Fig. S5), passivating the imperfections and enhancing the crystallization at the bottom of P(VDF-TrFE) films. Thus, the aligned dipole moments of the P(VDF-TrFE) copolymers on the CF_4-plasma-treated piezoelectric pressure sensors are significantly enhanced, inducing more electrons on the IGZO channel and thus resulting in the enhanced current response in Fig. 5(c) and (d).

4. Conclusion

In this study, the piezoelectric pressure sensors with high-density and low-damage CF_4-plasma-treated IGZO TFTs coated by P(VDF-TrFE) copolymers were developed. The plasma-fluorinated IGZO films and fluorine-incorporated P(VDF-TrFE) copolymers are identified using SIMS depth profiling, XPS characterization, XRD analysis, and AFM imaging. By examining the I_{DS}–V_{BG} curves of the plasma-fluorinated IGZO TFTs, an enhancement in μ_{FE} and I_{DS} and a negative shift in V_t are found due to an increase in oxygen vacancies of IGZO films and the reduction in the interfacial and oxide charges of SiO_2 layer, respectively. In addition, a drain current response multiplied by a factor of 4.8 under a 0.5-kg force applied on P(VDF-TrFE) copolymers is obtained for the plasma-fluorinated piezoelectric pressure sensors. The high-density and low-damage CF_4-plasma-treated IGZO TFTs with the P(VDF-TrFE) film coated on the topside of IGZO channel offer a piezoelectric pressure sensing device for the high-performance tactile sensing that can be integrated into robotic skin.

CRediT authorship contribution statement

Jer-Chyi Wang: Conceptualization, Methodology, Writing - review & editing, Supervision. **Yi-Pei Jiang:** Investigation, Validation, Data curation, Writing - original draft. **Chi-Hung Lin:** Investigation. **Shun-Hsiang Chan:** Investigation. **Ming-Chung Wu:** Methodology, Resources, Supervision.

Declaration of Competing Interest

No conflict of interest exits in the submission of this manuscript, and manuscript is approved by all authors for publication.

Acknowledgements

This research was supported by Ministry of Science and Technology, R.O.C. (Contract Nos. of MOST 107-2218-E-182-007 and MOST 108-2218-E-182-003) and Chang Gung Memorial Hospital, Linkou, Taiwan (Contract Nos. of CMRPD2H0132, CMRPD2J0051, and BMRPA74).

Appendix A. Supplementary data

Supplementary material related to this article can be found, in the online version, at doi:https://doi.org/10.1016/j.sna.2020.111855.

References

[1] C. Dagdeviren, P. Joe, O.L. Tuzman, K.-Il Park, K.J. Lee, Y. Shi, Y. Huang, J.A. Rogers, Recent progress in flexible and stretchable piezoelectric devices for mechanical energy harvesting, sensing and actuation, Extreme Mech. Lett. 9 (2016) 269–281.
[2] A.C. Turkmen, C. Celik, Energy harvesting with the piezoelectric material integrated shoe, Energy 150 (2018) 556–564.

[3] M.T. Chorsi, E.J. Curry, H.T. Chorsi, R. Das, J. Baroody, P.K. Purohit, H. Ilies, T.D. Nguyen, Piezoelectric biomaterials for sensors and actuators, Adv. Mater. 31 (2019), 1802084.
[4] K. Maity, D. Mandal, All-organic high-performance piezoelectric nanogenerator with multilayer assembled electrospun nanofiber mats for self-powered multifunctional sensors, ACS Appl. Mater. Interfaces 10 (2018) 18257–18269.
[5] P. Chevallier, Piezo-electric Cigarette Lighter, US patent, 1974, US3824063A, 16 July.
[6] H. Khanbareh, K. de Boom, B. Schelen, R.B.N. Scharff, C.C.L. Wang, S. van der Zwaag, P. Groen, Large area and flexible micro-porous piezoelectric materials for soft robotic skin, Sens. Actuator A-Phys. 263 (2017) 554–562.
[7] A. Sultana, S.K. Ghosh, V. Sencadas, T. Zheng, M.J. Higgins, T.R. Middyaa, D. Mandal, Human skin interactive self-powered wearable piezoelectric bio-e-skin by electrospun poly-L-lactic acid nanofibers for non-invasive physiological signal monitoring, J. Mater. Chem. B Mater. Biol. Med. 5 (2017) 7352–7359.
[8] B.-J. Lee, C.-W. Lee, Sound generation in decoupled acoustic guitar using electro-dynamic actuator, 13Th Asia Pacific Vibration Conference (2009) 1–10.
[9] K. Spanner, B. Koc, Piezoelectric motors, an overview, Actuators 5 (2016) 6.
[10] Q. Guo, G.Z. Cao, I.Y. Shen, Measurements of piezoelectric coefficient d_{33} of lead zirconate titanate thin films using a mini force hammer, J. Vib. Acoust. 135 (2013), 011003.
[11] B. Stadlober, M. Zirkla, M. Irimia-Vladu, Route towards sustainable smart sensors: ferroelectric polyvinylidene fluoride-based materials and their integration in flexible electronics, Chem. Soc. Rev. 48 (2019) 1787–1825.
[12] L. Ruan, X. Yao, Y. Chang, L. Zhou, G. Qin, X. Zhang, Properties and applications of the β Phase poly(vinylidene fluoride), Polymers 10 (2018) 228.
[13] R. Gregorio Jr, M.M. Botta, Effect of crystallization temperature on the phase transitions of P(VDF/TrFE) copolymers, J. Polym. Sci. Pt. B-Polym. Phys. 36 (1998) 403–414.
[14] K. Tashiro, K. Takano, M. Kobayashi, Y. Chatani, H. Tadokoro, Structural study on ferroelectric phase transition of vinylidene fluoride-trifluoroethylene copolymers (III) dependence of transitional behavior on VDF molar content, Ferroelectrics 57 (1984) 297–326.
[15] D. Mao, B.E. Gnade, M.A. Quevedo-Lopez, Ferroelectric properties and polarization switching kinetic of poly (vinylidene fluoride-trifluoroethylene) copolymer, Ferroelectrics - Physical effects (2011) 77–100, Chapter 4.
[16] U. Valiyaneerilakkal, S. Varghese, Poly (vinylidene fluoride-trifluoroethylene)/barium titanate nanocomposite for ferroelectric nonvolatile memory devices, AIP Adv. 3 (2013), 042131.
[17] A. Jain, S.J. Kumar, D.R. Mahapatra, V.T. Rathod, Development of P(VDF-Trfe) films and its quasi-static and dynamic strain response, Int. J. Eng. Res. Technol. Ahmedabad (Ahmedabad) 2 (2013) 2598–2605.
[18] K. Tashiro, Crystal structure and phase transition of PVDF and related copolymers, in: Ferroelectric Polymers Chemistry, Physics, and Applications, 1995, pp. 63–181, Chapter 2.
[19] J. Hu, J. Zhang, Z. Fu, Y. Jiang, S. Ding, G. Zhu, Solvent vapor annealing of ferroelectric P(VDF-TrFE) thin films, ACS Appl. Mater. Interfaces 6 (2014) 18312–18318.
[20] D. Singh, A. Deepak, Garg, Interface morphology driven control of electrical properties of P(VDF-TrFE) and PMMA blend M-I-M capacitors, Org. Electron. 15 (2014) 3811–3817.
[21] Z. Li, X. Zhang, G. Li, In situ ZnO nanowire growth to promote the PVDF piezo phase and the ZnO-PVDF hybrid self-rectified nanogenerator as a touch sensor, Phys. Chem. Chem. Phys. 16 (2014) 5475–5479.
[22] T. Zhou, J.-W. Zha, R.-Y. Cui, B.-H. Fan, J.-K. Yuan, Z.-M. Dang, Improving dielectric properties of BaTiO3/ferroelectric polymer composites by employing surface hydroxylated BaTiO3 nanoparticles, ACS Appl. Mater. Interfaces 3 (2011) 2184–2188.
[23] N. Tsutsumi, R. Kosugi, K. Kinashi, W. Sakai, Nature of the enhancement in ferroelectric properties by gold nanoparticles in vinylidene fluoride and trifluoroethylene copolymer, ACS Appl. Mater. Interfaces 8 (2016) 16816–16822.
[24] W. Park, J.H. Yang, C.G. Kang, Y.G. Lee, H.J. Hwang, C. Cho, S.K. Lim, S.C. Kang, W.-K. Hong, S.K. Lee, S. Lee, B.H. Lee, Characteristics of a pressure sensitive touch sensor using a piezoelectric PVDF-TrFE/MoS_2 stack, Nanotechnology 24 (2013), 475501.
[25] J.H. Yang, H.J. Hwang, S.C. Kang, B.H. Lee, Sensitivity improvement of graphene/Al_2O_3/PVDF–TrFE stacked touch device through Al seed assisted dielectric scaling, Microelectron. Eng. 147 (2015) 79–84.
[26] W. Li, J.A. Weldon, Y. Huang, K. Wang, Design and simulation of piezoelectric-charge-gated thin-film transistor for tactile sensing, IEEE Electron Device Lett. 37 (2016) 325–328.
[27] C.J. Chiu, S.P. Chang, S.J. Chang, High-performance amorphous indium–gallium–zinc oxide thin-film transistors with polymer gate dielectric, Thin Solid Films 520 (2012) 5455–5458.
[28] H.-C. Wu, C.-H. Chien, Highly transparent, high-performance IGZO-TFTs using the selective formation of IGZO source and drain electrodes, IEEE Electron Device Lett. 35 (2014) 645–647.
[29] I.-K. Lee, S.-W. Lee, J.-G. Gu, K.-S. Kim, W.-J. Cho, Comparative study of device performance and reliability in amorphous InGaZnO thin-film transistors with various high-k gate dielectrics, J. Appl. Phys. 52 (2013), 06GE05.
[30] M.H. Cho, H. Seol, H. Yang, P.S. Yun, J.U. Bae, K.-S. Park, J.K. Jeong, High-performance amorphous indium gallium zinc oxide thin-film transistors fabricated by atomic layer deposition, IEEE Electron Device Lett. 39 (2018) 688–691.
[31] J. Chen, H. Ning, Z. Fang, R. Tao, C. Yang, Y. Zhou, R. Yao, M. Xu, L. Wang, J. Peng, Reduced contact resistance of a-IGZO thin film transistors with inkjet-printed silver electrodes, J. Phys. D Appl. Phys. 51 (2018), 165103.
[32] J. Kim, S. Bang, S. Lee, S. Shin, J. Park, H. Seo, H. Jeon, A study on H_2 plasma treatment effect on a-IGZO thin film transistor, J. Mater. Res. 27 (2012) 2318–2325.
[33] J. Park, S. Kim, C. Kim, S. Kim, I. Song, H. Yin, K.-K. Kim, S. Lee, K. Hong, J. Lee, J. Jung, E. Lee, K.-W. Kwon, Y. Park, High-performance amorphous gallium indium zinc oxide thin-film transistors through N_2O plasma passivation, Appl. Phys. Lett. 93 (2008), 053505.
[34] J.-S. Park, J.K. Jeong, Y.-G. Mo, H.D. Kim, Improvements in the device characteristics of amorphous indium gallium zinc oxide thin-film transistors by Ar plasma treatment, Appl. Phys. Lett. 90 (2007), 262106.
[35] X.D. Huang, J.Q. Song, P.T. Lai, Improved stability of α-InGaZnO thin-film transistor under positive gate bias stress by using fluorine plasma treatment, IEEE Electron Device Lett. 38 (2017) 576–579.
[36] A. Bogaerts, E.C. Neyts, Plasma technology: an emerging technology for energy storage, ACS Energy Lett. 3 (2018) 1013–1027.
[37] J.H. Choi, S.J. Kim, H.T. Kim, S.M. Cho, Damage to amorphous indium-gallium-zinc-oxide thin film transistors under Cl_2 and BCl_3 plasma, Korean J. Chem. Eng. 35 (2018) 1348–1353.
[38] C.-H. Huang, C.-T. Lin, J.-C. Wang, C. Chou, Y.-R. Ye, B.-M. Cheng, C.-S. Lai, Tunable bandgap energy of fluorinated nanocrystals for flash memory applications produced by low-damage plasma treatment, Nanotechnology 23 (2012), 475201.
[39] J.H. Yang, T. Ryu, Y. Lansac, Y.H. Jang, B.H. Lee, Shear stress-induced enhancement of the piezoelectric properties of PVDF-TrFE thin films, Org. Electron. 28 (2016) 67–72.
[40] J. Wang, Z. Li, Y. Yan, X. Wang, Y.C. Xie, Z.C. Zhang, Improving ferro- and piezo- electric properties of hydrogenized poly(vinylidene fluoride-trifluoroethylene) films by annealing at elevated temperatures, Chin. J. Polym. Sci. 34 (2016) 649–658.
[41] W.-G. Kim, Y.J. Tak, B.D. Ahn, T.S. Jung, K.-B. Chung, H.J. Kim, High-pressure gas activation for amorphous indium-gallium-zinc-oxide thin-film transistors at 100 °C, Sci. Rep. 6 (2016) 23039.
[42] J. Zhang, X. Wen, L. Hu, W. Xu, D. Zhu, P. Cao, W. Liu, S. Han, X. Liu, F. Jia, Y. Zeng, Y. Lu, C-Axis oriented crystalline IGZO thin-film transistors by magnetron sputtering, J. Mater. Chem. C Mater. Opt. Electron. Devices 5 (2017) 2388–2396.
[43] J. Chen, L. Wang, X. Su, L. Kong, G. Liu, X. Zhang, InGaZnO semiconductor thin film fabricated using pulsed laser deposition, Opt. Express 18 (2010) 1398–1405.
[44] J.H. Choi, J.H. Shim, S.M. Hwang, J. Joo, K. Park, H. Kim, H.-J. Lee, Effect of sintering time at low temperature on the properties of IGZO TFTs fabricated by using the sol-gel process, J. Korean Phys. Soc. 57 (2010) 1836–1841.
[45] https://srdata.nist.gov/xps/EnergyTypeValSrch.aspx.
[46] J.K. Um, S. Lee, S. Jin, M. Mativenga, S.Y. Oh, C.H. Lee, J. Jang, High-performance homojunction a-IGZO TFTs with selectively defined low-resistive a-IGZO source/drain electrodes, IEEE Trans. Electron Devices 62 (2015) 2212–2218.
[47] Y. Lei, K. Ng, L. Weng, C. Chan, L. Li, XPS C 1s binding energies for fluorocarbon–hydrocarbon microblock copolymers, Surf. Interface Anal. 35 (2003) 852–855.
[48] A.V. Solnyshkin, D.A. Kiselev, A.A. Bogomolov, A.L. Kholkin, W. Künstler, R. Gerhard, Atomic force microscopy study of ferroelectric films of P(VDF–TrFE) copolymer and composites based on it, J. Surf. Ingestig.-X-Ray Synchro. 2 (2008) 692–695.
[49] T. Feng, D. Xie, Y. Zang, X. Wu, T. Ren, W. Pan, Temperature control of P(VDF-TrFE) copolymer thin films, Integr. Ferroelectr. 141 (2013) 187–194.
[50] E. Chong, Y.S. Chun, S.H. Kim, S.Y. Lee, Effect of oxygen on the threshold voltage of a-IGZO TFT, J. Electr. Eng. Technol. 6 (2011) 539–542.
[51] J. Lee, J.-S. Park, Y.S. Pyo, D.B. Lee, E.H. Kim, D. Stryakhilev, T.W. Kim, D.U. Jin, Y.-G. Mo, The influence of the gate dielectrics on threshold voltage instability in amorphous indium-gallium-zinc oxide thin film transistors, Appl. Phys. Lett. 95 (2009), 123502.
[52] W.-P. Zhang, S. Chen, S.-B. Qian, S.-J. Ding, Effects of thermal annealing on the electrical characteristics of In-Ga-Zn-O thin-film transistors with Al_2O_3 gate dielectric, Semicond. Sci. Technol. 30 (2015), 015003.
[53] R.S. Dahiya, M. Valle, Robotic Tactile Sensing: Technologies and System, 1st ed., Springer-Verlag, NY, 2012, pp. 235.
[54] N. Yogeswaran, W.T. Navaraj, S. Gupta, F. Liu, V. Vinciguerra, L. Lorenzelli, R. Dahiya, Piezoelectric graphene field effect transistor pressure sensors for tactile sensing, Appl. Phys. Lett. 113 (2018), 014102.

Biographies

Jer-Chyi Wang received the B.Sc. and Ph.D. degrees from National Chiao-Tung University, Hsinchu, Taiwan, in 1998 and 2003, respectively. In 2003, he joined the Nanya Technology Corporation, Taoyuan, Taiwan, where he has been engaged in the research on dynamic random access memory. He was promoted as a process and device simulation section manager in 2008. Since 2009, he joined the Department of Electronic Engineering, Chang Gung University, Taoyuan, Taiwan, as an Assistant Professor. He was promoted to a Professor in 2015, where he has been engaged in

the research of characteristics and reliability of MOSFETs, metal-gate/high-k technology, advanced memory device fabrication, 3-D process and device simulation, and bio-sensor device fabrication and applications.

Yi-Pei Jiang received the B.Sc. in the Department of Electronic Engineering from Chang Gung University, Taoyuan, Taiwan in 2015. Her research interests include solid-state devices and pressure sensors. Her focuses are on the development of thin film transistor, ferroelectric and piezoelectric sensing membranes with plasma treatment and light-induced process to investigate the enhancement of the device characteristics.

Chi-Hung Lin received the M.S. degree from Department of Chemical and Materials Engineering, Chang Gung University in 2018 with a research interest of developing VOCs sensors.

Shun-Hsiang Chan received his M.S. and Ph.D. degrees from Department of Chemical and Materials Engineering of Chang Gung University, Taiwan, in 2014 and 2018, respectively. His main research interests include next-generation solar cells, nanomaterials, polymer composites, and optical gas sensors. He has published 17 SCI papers and has been awarded 1 Taiwanese patent.

Ming-Chung Wu received the M.Sc. and Ph.D. degrees from National Taiwan University, Taipei, Taiwan, in 2004 and 2008, respectively. In 2009, he joined Department of Electrical and Information Engineering, University of Oulu, Finland, as a Postdoctoral Researcher. Since 2012, he joined the Department of Chemical and Materials Engineering, Chang Gung University, Taoyuan, Taiwan, as an Assistant Professor. He was promoted to an Associate Professor in 2015, where he has been engaged in the research of advanced energy materials, nanomaterials and nanotechnology, optoelectronic materials, and devices physics.